RHEUMATOLOGY

Rheumatology 2023;62:SI125–SI137
https://doi.org/10.1093/rheumatology/keac433
Advance access publication 28 July 2022

Original article

Soluble guanylate cyclase stimulation fosters angiogenesis and blunts myofibroblast-like features of systemic sclerosis endothelial cells

Eloisa Romano[1,*], Irene Rosa[2,*], Bianca Saveria Fioretto[1,2], Dilia Giuggioli[3], Mirko Manetti[2,†] and Marco Matucci-Cerinic[1,4,†]

Abstract

Objectives. In SSc, angiogenesis impairment advances in parallel with the development of fibrosis orchestrated by myofibroblasts originating from different sources, including endothelial-to-mesenchymal transition (EndoMT). Soluble guanylate cyclase (sGC) stimulation has shown antifibrotic effects in SSc skin fibroblasts and mouse models. Here, we investigated the effects of pharmacological sGC stimulation on impaired angiogenesis and myofibroblast-like features of SSc dermal microvascular endothelial cells (SSc-MVECs).

Methods. To determine whether sGC stimulation affected cell viability/proliferation, SSc-MVECs and healthy dermal MVECs (H-MVECs) were challenged with the sGC stimulator (sGCS) MK-2947 and assayed by annexin V/propidium iodide flow cytometry and the water-soluble tetrazolium salt (WST-1) assay. To study angiogenesis and EndoMT, MK-2947-treated SSc-MVECs were subjected to wound healing and capillary morphogenesis assays and analysed for the expression of endothelial/myofibroblast markers and contractile ability.

Results. MK-2947 treatment did not affect H-MVEC viability/proliferation, while it significantly increased SSc-MVEC proliferation, wound healing capability and angiogenic performance. After MK-2947 treatment, SSc-MVECs exhibited significantly increased proangiogenic *MMP9* and decreased antiangiogenic *MMP12* and *PTX3* gene expression. A significant increase in the expression of CD31 and vascular endothelial cadherin paralleled by a decrease in α-smooth muscle actin, S100A4, type I collagen and Snail1 mesenchymal markers was also found in MK-2947-treated SSc-MVECs. Furthermore, stimulation of sGC with MK-2947 significantly counteracted the intrinsic ability of SSc-MVECs to contract collagen gels and reduced phosphorylated-extracellular signal-regulated kinases 1 and 2 protein levels.

Conclusion. These findings demonstrate for the first time that pharmacological sGC stimulation effectively ameliorates the angiogenic performance and blunts the myofibroblast-like profibrotic phenotype of SSc-MVECs, thus providing new evidence for repurposing sGCSs for SSc.

Key words: SSc, endothelial cells, angiogenesis, endothelial-to-mesenchymal transition, soluble guanylate cyclase

Rheumatology key messages

- Soluble guanylate cyclase stimulation ameliorates the impaired angiogenic performance of SSc dermal microvascular endothelial cells.
- Soluble guanylate cyclase stimulation blunts the myofibroblast-like profibrotic behaviour of SSc dermal microvascular endothelial cells.
- Soluble guanylate cyclase stimulation protects healthy endothelial cells against TGFβ- and SSc serum-induced endothelial-to-mesenchymal transition.

[1]Department of Experimental and Clinical Medicine, Division of Rheumatology, [2]Department of Experimental and Clinical Medicine, Section of Anatomy and Histology, University of Florence, Florence, [3]Department of Medical and Surgical Sciences for Children and Adults, Scleroderma Unit, University of Modena and Reggio Emilia, Modena and [4]Unit of Immunology, Rheumatology, Allergy and Rare Diseases (UnIRAR), IRCCS San Raffaele Hospital, Milan, Italy

Submitted 10 May 2022; accepted 19 July 2022

Correspondence to: Mirko Manetti, Department of Experimental and Clinical Medicine, Section of Anatomy and Histology, University of Florence, 50134 Florence, Italy. E-mail: mirko.manetti@unifi.it

*Eloisa Romano and Irene Rosa contributed equally to this study.

†Mirko Manetti and Marco Matucci-Cerinic contributed equally to this study.

BASIC SCIENCE

Introduction

SSc is a connective tissue disease characterized by microvascular damage, immune activation, and skin and internal organ fibrosis [1–3]. Peripheral microvascular abnormalities are the earliest SSc manifestations, with the endothelium representing one of the major disease targets and, possibly, a trigger for the subsequent development of vascular and tissue fibrosis accompanied by progressive capillary rarefaction due to the lack of compensatory angiogenesis [1–3]. Indeed, it has been shown that dermal microvascular endothelial cells (MVECs) from the involved skin of patients with diffuse cutaneous SSc (SSc-MVECs) exhibit an impaired angiogenic potential [3–6] and can transdifferentiate into profibrotic myofibroblasts through endothelial-to-mesenchymal transition (EndoMT) [7], thus taking an active part in both SSc-related fibroproliferative/destructive vasculopathy and tissue fibrosis [8, 9].

Soluble guanylate cyclase (sGC) catalyses the production of cyclic guanosine monophosphate (cGMP) upon binding of nitric oxide (NO) to its prosthetic haem group [10]. Once released, cGMP can act as second messenger to activate different downstream targets regulating physiological processes including cell growth/proliferation, vascular tone and remodelling, and immune responses [10–11]. Two different types of pharmaceutical molecules have been developed to enhance sGC activity, namely sGC activators and sGC stimulators (sGCSs) [12]. The former bind to the oxidized, haem-free and NO-unresponsive form of sGC [13], while sGCSs stimulate the reduced, haem-containing native form of the enzyme independently of NO, being also able to sensitize sGC to low levels of NO by stabilizing NO–sGC binding [10, 12]. The therapeutic potential effect of augmenting cGMP production has been reported in several studies. Indeed, the increase in sGC activity has been shown to lower blood pressure and to exert anti-inflammatory and antifibrotic effects in experimental models of various diseases [10, 13]. In particular, the administration of the sGC activator BAY 60-277 attenuated liver fibrosis in different rat models [14, 15], while treatment with the sGCS BAY 41-2272 decreased experimental hepatic, peritoneal and cardiac fibrosis [16–18] and significantly lessened TGFβ-induced fibroblast proliferation and fibroblast-to-myofibroblast differentiation [19, 20]. As for SSc, treatment with BAY 41-2272 was reported to inhibit collagen release in dermal fibroblasts by interfering with a non-canonical TGFβ cascade and to rest the development of skin fibrosis in both the bleomycin-induced and Tsk-1 mouse models of SSc [21, 22]. Another sGCS, named riociguat, was also effective in decreasing collagen deposition, skin thickening and myofibroblast accumulation in the same experimental SSc murine models [23]. Moreover, riociguat was shown to ameliorate oesophageal and intestinal profibrotic response in the bleomycin-induced mouse model [24]. Clinically, the pharmacological use of sGCS compounds has been proved to ameliorate both symptomatic chronic heart failure [12, 25] and different forms of pulmonary hypertension [10, 12, 26, 27]. Specifically, riociguat demonstrated vasodilatory, antiproliferative, vascular remodelling, antifibrotic and anti-inflammatory effects in several preclinical studies [23, 28–30], and was effective for the treatment of patients with different forms of pulmonary hypertension, including SSc-related pulmonary arterial hypertension (PAH) [31–33]. Riociguat efficacy was also investigated in patients with diffuse cutaneous SSc in a placebo-controlled phase 2 study in which a tendency towards a reduction of Raynaud's phenomenon symptoms and attack frequency after treatment was observed [34]. In another multicentre trial on SSc patients with active or painful digital ulcers (DUs), riociguat was not able to reduce the number of DUs when compared with placebo, but a trend towards DU healing was reported after longer treatment, suggesting that extended duration of treatment with such compounds should be investigated in further clinical trials [26].

On these premises, the aim of our *in vitro* research was to unravel whether sGC stimulation could modulate the angiogenic performance and the intrinsic myofibroblast-like profibrotic behaviour of SSc-MVECs explanted from the clinically affected skin of patients with the early diffuse cutaneous form of the disease.

Methods

See Supplementary Data S1, available at *Rheumatology* online, for detailed methodology.

Patients and serum samples

Serum samples and forearm skin biopsies were obtained from five patients with early diffuse cutaneous SSc (disease duration <2 years from first non-Raynaud symptom) fulfilling the ACR/EULAR 2013 classification criteria [35] and recruited from the Division of Rheumatology, Azienda Ospedaliero-Universitaria Careggi, Florence, Italy. The study was conducted in accordance with the Declaration of Helsinki, and approved by the Comitato Etico Regionale per la Sperimentazione Clinica della Toscana—sezione AREA VASTA CENTRO, Florence, Italy (approval number: 18559/bio; approval date: 13 April 2021). Participants gave written informed consent before taking part in the study. Demographic and clinical features of SSc patients are shown in Supplementary Table S1, available at *Rheumatology* online.

Cell culture and reagents

Five lines of adult human dermal MVECs (H-MVECs) were purchased from Lonza, while primary cultures of SSc-MVECs were obtained from skin biopsies of SSc patients ($n = 5$). Cells were administered with the sGCS MK-2947 (Merck Sharp & Dohme, Kenilworth, NJ, USA) 1 μM or 10 μM before being assayed. In selected experiments, H-MVECs were treated with recombinant human TGFβ (10 ng/ml; PeproTech, Rocky Hill, NJ,

USA) or 10% serum from SSc patients ($n = 5$) for 48 h, or preincubated for 2 h with MK-2947 10 μM before being challenged with TGFβ or SSc sera. For more details, see Supplementary Data S1, available at *Rheumatology* online.

Annexin V/propidium iodide flow cytometry assay

H-MVECs and SSc-MVECs were challenged with MK-2947 1 μM or 10 μM for 48 h and assayed for annexin V/propidium iodide (PI) staining by flow cytometry assay as detailed in Supplementary Data S1, available at *Rheumatology* online.

Cell proliferation assay

H-MVECs and SSc-MVECs were stimulated with MK-2947 1 μM or 10 μM for 48 h and assayed by water-soluble tetrazolium salt (WST-1) assay as detailed in Supplementary Data S1, available at *Rheumatology* online.

In vitro wound healing assay

A wound healing assay was performed on confluent SSc-MVECs incubated with MK-2947 1 μM or 10 μM and H-MVECs stimulated with MK-2947 10 μM for 24 and 48 h as described in Supplementary Data S1, available at *Rheumatology* online. Wound healing capacity was assessed by capturing phase-contrast images of the wounded area under a Leica inverted microscope (Leica Microsystems, Mannheim, Germany). Images at 0 and 48 h for each experimental point were compared to quantify the migration rate of the cells after wounding.

In vitro capillary-like tube formation assay

In vitro angiogenesis was performed on SSc-MVECs challenged with MK-2947 1 μM or 10 μM and H-MVECs stimulated with MK-2947 10 μM. Angiogenesis was assessed with the angiogenesis analyser tool of ImageJ software (NIH, Bethesda, MD, USA). For more details, see Supplementary Data S1, available at *Rheumatology* online.

RNA purification, cDNA synthesis and quantitative real-time PCR

SSc-MVECs were stimulated with MK-2947 1 μM or 10 μM for 48 h before RNA purification. RNA was also purified from H-MVECs treated with TGFβ (10 ng/ml) or 10% SSc serum for 48 h, or preincubated for 2 h with MK-2947 10 μM before being challenged with TGFβ or SSc sera. Predesigned oligonucleotide primer pairs for *VEGF*, *MMP9*, *MMP12*, *PTX3*, *CD31*, *CDH5*, *ACTA2*, *S100A4*, *COL1A1*, *COL1A2*, *SNAI1* and *RRN18S* were obtained from Qiagen (Qiagen, Milan, Italy). For more details, see Supplementary Data S1, available at *Rheumatology* online.

Immunoblotting

H-MVECs were challenged with MK-2947 10 μM, while SSc-MVECs were stimulated with MK-2947 1 μM or 10 μM for 72 h before preparation of whole cell protein lysates according to previously published procedures [6]. Primary antibodies against CD31, vascular endothelial (VE)-cadherin, α-smooth muscle actin (α-SMA), S100A4/fibroblast-specific protein-1, type I collagen, Snail1, extracellular signal-regulated kinases 1 and 2 (ERK1/2), phosphorylated-ERK1/2, Ki67, α-tubulin and glyceraldehyde 3-phosphate dehydrogenase were employed. Further details are provided in Supplementary Data S1, available at *Rheumatology* online.

Immunofluorescence

SSc-MVECs were seeded onto glass coverslips and treated with MK-2947 1 μM or 10 μM for 72 h. Cells were fixed and incubated with primary antibodies against CD31, VE-cadherin, α-SMA, S100A4, type I collagen or Snail1 as detailed in Supplementary Data S1, available at *Rheumatology* online. Immunostained cells were examined with a Leica DM4000 B microscope (Leica Microsystems) and fluorescence images were captured with a Leica DFC310 FX 1.4-megapixel digital colour camera equipped with the Leica software application suite LAS V3.8 (Leica Microsystems).

Collagen gel contraction assay

Collagen gel contraction assays were performed using the CytoSelect 24-Well Cell Contraction Assay Kit (Cell Biolabs, San Diego, CA, USA) as detailed in Supplementary Data S1, available at *Rheumatology* online. SSc-MVECs were treated with MK-2947 1 μM or 10 μM for 48 h before the assay. After 24 h, the culture dish was scanned and the area of each collagen gel was measured by ImageJ software (NIH).

Statistical analysis

Statistical analysis was performed using the SPSS Statistics for Windows, version 27.0 (IBM Corp, Armonk, NY, USA). Data are expressed as mean ± (S.E.M.). One-way ANOVA with *post hoc* Tukey's test was used for statistical analyses. $P < 0.05$ was considered statistically significant.

Results

Treatment with the sGCS MK-2947 does not induce MVEC apoptosis/necrosis and fosters SSc-MVEC proliferation

We first investigated whether sGC stimulation could boost the proliferation of SSc-MVECs, whose impairment is known to contribute to defective angiogenesis [6]. To inspect for any possible side effects of treatment with the sGCS MK-2947 (1 and 10 μM), cell viability and proliferation of both H-MVECs and SSc-MVECs were

FIG. 1 Soluble guanylate cyclase stimulation does not induce endothelial cell apoptosis or necrosis and fosters SSc-MVEC proliferation

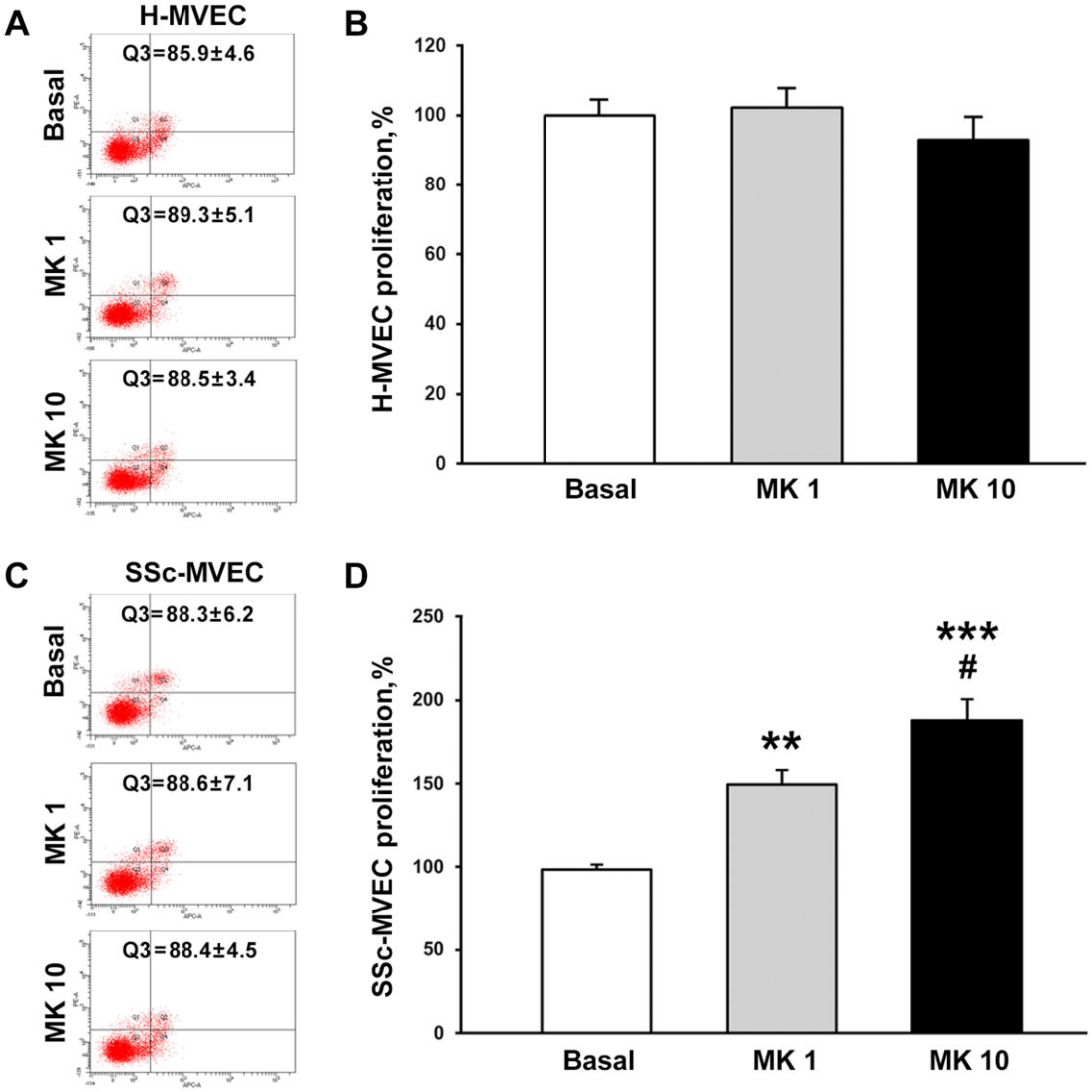

(**A**–**D**) Cell viability and proliferation were assessed at basal condition and after treatment with MK-2947 1 μM or 10 μM. (**A**, **C**) Representative annexin V/PI plots of H-MVECs ($n = 5$) (**A**) and SSc-MVECs ($n = 5$) (**C**). The mean (S.E.M.) percentage of viable cells is reported. (**B**, **D**) Proliferation of H-MVECs (**B**) and SSc-MVECs (**D**) assessed by WST-1 assay. Basal cell proliferation was set to 100%. Bars represent the mean (S.E.M.) of triplicate determinations. One-way ANOVA with *post hoc* Tukey's test was used for statistical analysis; $^{**}P < 0.01$ and $^{***}P < 0.001$ *vs* basal, $^{\#}P < 0.05$ *vs* MK-2947 1 μM. H-MVEC: healthy MVEC; MVEC: microvascular endothelial cell; PI: propidium iodide; WST-1: water-soluble tetrazolium salt.

determined by annexin V/PI flow cytometry and WST-1, respectively. Indeed, the annexin V/PI assay is used to determine whether cells are viable, apoptotic or necrotic through differences in plasma membrane integrity and permeability, while the WST-1 assay allows evaluation of proliferation by measuring cell metabolism. In H-MVECs, treatment with MK-2947 at both concentrations did not alter cell viability (Fig. 1A). Moreover, treatment with MK-2947 did not influence proliferation of H-MVECs (Fig. 1B). As far as SSc-MVECs are concerned, cell viability was not different between cells treated with MK-2947 1 μM or 10 μM and untreated cells (Fig. 1C), while stimulation with the sGCS resulted in a significant increase in cell proliferation at both concentrations compared with untreated cells, reaching a maximum at 10 μM ($P < 0.01$ for MK-2947 1 μM and $P < 0.001$ for MK-2947 10 μM, Fig. 1D). Of note, stimulation of SSc-MVECs with MK-2947 10 μM was not able to fully

FIG. 2 Soluble guanylate cyclase stimulation increases wound healing capacity of SSc-MVECs

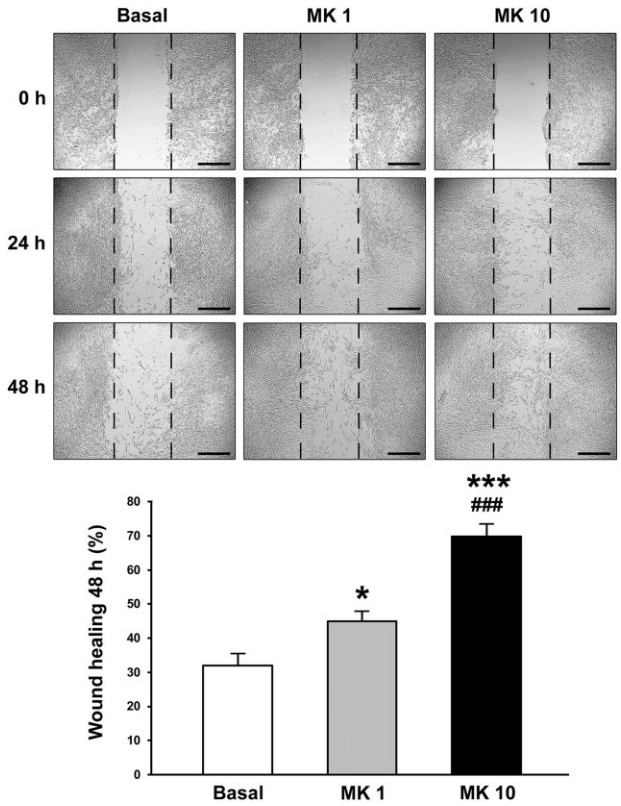

Wound healing assay was performed on SSc-MVECs ($n = 5$) at basal condition and after stimulation with MK-2947 1 μM or 10 μM. Representative phase-contrast images of the wound at 0, 24 and 48 h after scratching are shown; dashed lines represent wound margins. Scale bar = 200 μm. Bar graph represents quantitative analysis of the percentage of healing after 48 h. Bars represent the mean (S.E.M.) of triplicate determinations. One-way ANOVA with *post hoc* Tukey's test was used for statistical analysis; $^{*}P < 0.05$ and $^{***}P < 0.001$ *vs* basal, $^{\#\#\#}P < 0.001$ *vs* MK-2947 1 μM. MVEC: microvascular endothelial cell.

restore cell proliferation rate to that of basal H-MVECs (Supplementary Fig. S1A, available at *Rheumatology* online). Consistent with these findings, when we investigated if MK-2947 administration could modulate Ki67 expression, we found that protein levels of this proliferative marker were significantly higher in MK-2947 10 μM-treated SSc-MVECs with respect to untreated SSc cells, but without reaching those of basal H-MVECs (Supplementary Fig. S1B, available at *Rheumatology* online).

MK-2947 increases the wound healing capacity of SSc-MVECs

The wound healing capacity of SSc-MVECs is known to be profoundly compromised as a result of defective cell migration and proliferation [6]. As shown in Fig. 2, the ability of SSc-MVECs to restore the monolayer integrity at 48 h after scratching was significantly ameliorated in a dose-dependent manner when cells were treated with MK-2947 ($P < 0.05$ for MK-2947 1 μM and $P < 0.001$ for MK-2947 10 μM *vs* basal; $P < 0.001$ for MK-2947 10 μM *vs* MK-2947 1 μM). However, stimulation of SSc-MVECs with the higher dose of MK-2947 was not able to completely restore wound healing ability to the level of basal H-MVECs (Supplementary Fig. S2, available at *Rheumatology* online).

Treatment with MK-2947 ameliorates capillary-like tube formation and modulates the expression of angiogenic regulators in SSc-MVECs

In vitro angiogenesis was assayed by seeding H-MVECs and SSc-MVECs on Geltrex matrix in the presence of MK-2947 1 μM or 10 μM. Capillary-like tube formation was examined after 24 h by quantifying the number of nodes (pixels with three neighbours), segments (tubes delimited by two junctions), meshes (regions enclosed by segments) and junctions (branching points). Compared with their basal condition, in which *in vitro* angiogenesis was severely impaired, the number of nodes, segments and junctions formed by SSc-MVECs significantly increased in the presence of MK-2947 at both 1 μM and 10 μM, while the number of meshes was significantly higher only with MK-2947 10 μM (Fig. 3A). A statistically significant difference between MK-2947 1 μM

FIG. 3 Soluble guanylate cyclase stimulation ameliorates the angiogenic performance and modulates the expression of angiogenic regulators in SSc-MVECs

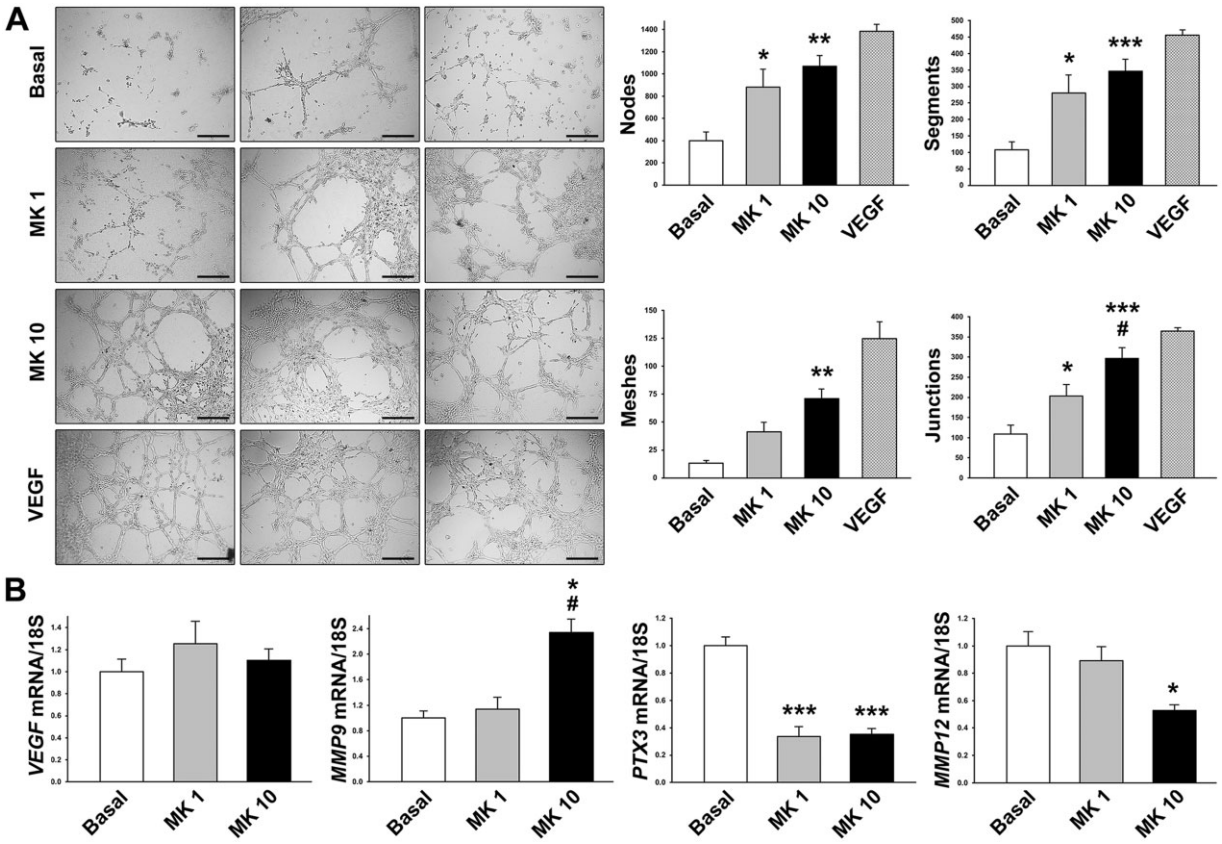

Experiments were performed on SSc-MVECs ($n = 5$) at basal condition and after treatment with MK-2947 1 μM or 10 μM. (**A**) *In vitro* capillary-like tube formation. VEGF stimulation was performed as positive control. Representative phase-contrast images after 24 h are shown. Scale bar = 200 μm. Bar graphs show the quantification of nodes, segments, meshes and junctions. (**B**) Gene expression of *VEGF*, *MMP9*, *PTX3* and *MMP12* assessed by quantitative real-time PCR. The basal level of each gene expression was set to 1. 18S rRNA was used as reference gene. Bars represent the mean (S.E.M.) of triplicate determinations. One-way ANOVA with *post hoc* Tukey's test was used for statistical analysis; $^{*}P < 0.05$, $^{**}P < 0.01$ and $^{***}P < 0.001$ *vs* basal, $^{\#}P < 0.05$ *vs* MK-2947 1 μM. MVEC: microvascular endothelial cell.

and 10 μM was found exclusively when considering the number of junctions (Fig. 3A). Notably, when treated with MK-2947 10 μM, SSc-MVECs showed an increase in the number of segments, meshes and junctions at levels similar to those of basal H-MVECs (Supplementary Fig. S3, available at *Rheumatology* online). Collectively, these data indicated that sGC stimulation was able to improve the angiogenic performance of SSc-MVECs.

To further investigate if stimulation with the sGCS could modulate the production of proangiogenic and antiangiogenic molecules known to be impaired in SSc [3], we performed gene expression analysis by quantitative real-time PCR. Treatment of SSc-MVECs with the higher concentration of the sGCS significantly augmented the expression levels of *MMP9* gene, while decreasing gene expression of both antiangiogenic *MMP12* and *PTX3* (Fig. 3B). Stimulation with MK-2947 1 μM was able to decrease only *PTX3* mRNA levels (Fig. 3B).

Treatment with MK-2947 attenuates the myofibroblast-like phenotype of SSc-MVECs

Previous studies demonstrated that cultured SSc-MVECs co-express endothelial and myofibroblast markers and display a myofibroblast-like profibrotic and contractile phenotype [7, 36]. Indeed, at variance with H-MVECs, SSc-MVECs synthesize elevated amounts of type I collagen and express high levels of α-SMA assembled into stress fibres, which makes them capable of contracting extracellular matrix [7]. To evaluate whether sGCS treatment could modify these intrinsic EndoMT features, SSc-MVECs challenged with MK-2947 1 μM or 10 μM were assayed for the expression of endothelial- and mesenchymal/myofibroblast-specific markers and for the ability to contract collagen gels. Quantitative real-time PCR analysis performed on SSc-MVECs challenged with MK-2947 10 μM revealed a

Fig. 4 Soluble guanylate cyclase stimulation attenuates the myofibroblast-like gene expression profile of SSc-MVECs

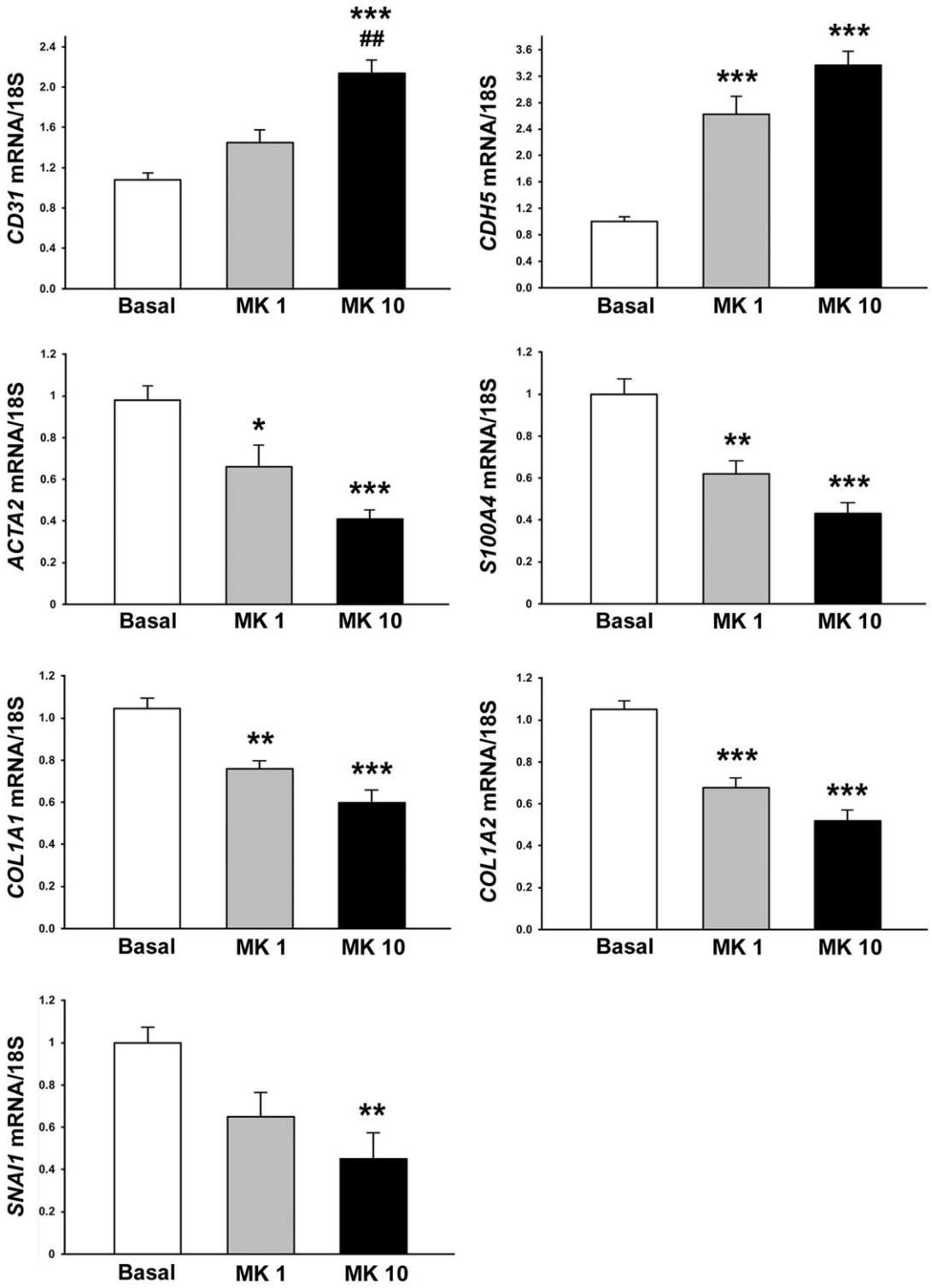

Gene expression of endothelial (*CD31* and *CDH5*) and mesenchymal/myofibroblast (*ACTA2*, *S100A4*, *COL1A1*, *COL1A2* and *SNAI1*) markers in SSc-MVECs ($n = 5$) at basal condition and after stimulation with MK-2947 1 μM or 10 μM was assessed by quantitative real-time PCR. The basal level of each gene expression was set to 1. 18S rRNA was used as reference gene. Bars represent the mean (S.E.M.) of triplicate determinations. One-way ANOVA with *post hoc* Tukey's test was used for statistical analysis; $^{*}P < 0.05$, $^{**}P < 0.01$ and $^{***}P < 0.001$ *vs* basal, $^{\#\#}P < 0.01$ *vs* MK-2947 1 μM. MVEC: microvascular endothelial cell.

significant increase in the expression of *CD31* and *CDH5* (gene encoding VE-cadherin) endothelial genes and a parallel decrease in the expression of *ACTA2* (gene encoding α-SMA), *S100A4*, *COL1A1*, *COL1A2* and *SNAI1* (gene encoding the transcription factor Snail1) mesenchymal genes (Fig. 4). Treatment of SSc-MVECs with MK-2947 1 μM was able to induce *CDH5* and to reduce *ACTA2*, *S100A4*, *COL1A1* and *COL1A2* mRNA (Fig. 4).

As far as protein expression is concerned, both CD31 and VE-cadherin were significantly increased in SSc-MVECs challenged with MK-2947 10 μM (Fig. 5A, B). VE-cadherin protein expression was also augmented after challenging with MK-2947 1 μM (Fig. 5B). Significantly lower protein levels of α-SMA, S100A4 and type I collagen were detected in SSc-MVECs after stimulation with MK-2947 at both 1 μM and 10 μM (Fig. 5C–E). Instead, Snail1 protein expression was significantly decreased only after treatment with MK-2947 10 μM (Fig. 5F). Similar findings were observed after immunofluorescence staining of SSc-MVECs for the same endothelial/myofibroblast markers (Fig. 5G). Treatment with the sGCS was also able to significantly counteract the intrinsic myofibroblast-like ability of SSc-MVECs to contract collagen gels ($P < 0.001$ for both MK-2947 concentrations *vs* basal, Fig. 5H).

Since it has previously been demonstrated that sGC stimulation may inhibit the profibrotic phenotype of SSc fibroblasts by blocking non-canonical ERK-dependent TGFβ signalling [21, 22], we assessed the effect of MK-2947 administration on ERK1/2 phosphorylation in SSc-MVECs. Treatment of SSc-MVECs with MK-2947 10 μM effectively reduced phosphorylated-ERK1/2 protein levels with respect to basal cells (Fig. 5I).

Administration of MK-2947 protects H-MVECs from EndoMT induced by treatment with TGFβ or SSc serum

We finally verified whether the sGCS could modulate the pro-EndoMT effects exerted on H-MVECs by recombinant human TGFβ or serum from SSc patients [7]. As displayed in Fig. 6, quantitative real-time PCR revealed significant reduction of *CDH5* and induction of *ACTA2*, *S100A4*, *COL1A1*, *COL1A2* and *SNAI1* gene expression in cells treated with TGFβ or SSc sera. Such pro-EndoMT effects were significantly blunted when H-MVECs were preincubated with MK-2947 (Fig. 6).

Discussion

This is to our knowledge the first study investigating the possible effects of pharmacological stimulation of sGC in modulating key pathological features of SSc-MVECs. Our data clearly demonstrated that treatment with the sGCS MK-2947 can ameliorate SSc-MVEC proliferative/migratory abilities, overall improving their scarce aptitude to perform angiogenesis. Moreover, MK-2947 was effective in attenuating the intrinsic myofibroblast-like phenotype of SSc-MVECs through the inhibition of non-canonical ERK-dependent TGFβ signalling. Of note, MK-2947 treatment also demonstrated efficacy in counteracting both TGFβ- and SSc serum-induced EndoMT in H-MVECs.

Since the early stages of SSc, microvascular abnormalities represent important pathological events that progressively stimulate the fibrotic process and can result in severe vascular complications, such as refractory ischaemic DUs and PAH [1–3]. Increasing evidence has demonstrated that SSc-MVECs are characterized by abnormal activation and the phenotypical switch towards profibrotic myofibroblasts known as EndoMT, becoming unable to perform angiogenesis and making an important contribution to both microvascular dysfunction and tissue fibrosis [7–9, 36–38]. Currently, few putative therapeutic options have been proposed to promote effective angiogenesis and counteract in parallel the EndoMT process in SSc [8, 9].

In this context our data demonstrated that sGC stimulation exerts pro-proliferative and pro-migratory effects on SSc-MVECs in a dose-dependent manner, and that it is able to ameliorate SSc-MVEC angiogenic properties by increasing their capability to form capillary-like tubular structures. These results are in line with previous studies reporting that sGC activation can promote different steps of the angiogenic process, such as endothelial cell proliferation, migration and tube formation [39–41]. Indeed, sGC activation was reported to stimulate new vessel formation in the chicken chorioallantoic membrane angiogenesis model [39]. Moreover, treatment of human umbilical vein endothelial cells (HUVECs) with the sGCS BAY 41-2272 led to an increase in cell proliferation and migration, while stimulation with a selective sGC inhibitor resulted in the formation of fewer capillary-like structures [40, 41]. Additionally, overexpression of sGC in HUVECs was shown to increase the proliferation rate, migratory capability and organization of cells into networks, thus mirroring the effects obtained using the pharmacological activation of the enzyme [39]. In another study, sGC inhibition with NS-2028 attenuated VEGF-induced proliferation and migration of HUVECs, and blocked VEGF-triggered microvessel formation in rat aortic ring explants [40]. In the same study, *in vivo* experiments on rabbits receiving NS-2028 showed a significant reduction of VEGF-induced new vessel formation in the avascular cornea [40]. Furthermore, circulating endothelial progenitor cells (EPCs) from patients with chronic thromboembolic pulmonary hypertension (CTEPH) and treated with riociguat exhibited enhanced angiogenic abilities compared with cells from untreated patients [41]. Co-culture of human pulmonary MVECs with EPCs from the riociguat group of patients resulted in increased cell migration and tube formation, suggesting that sGC stimulation may improve pulmonary neovascularization in CTEPH patients [41]. Finally, in a rat model of chronic pulmonary embolism, riociguat strongly increased pulmonary angiogenesis and ameliorated cardiac deficiencies [42], whereas in a mouse model of hindlimb ischaemia it increased capillary density [43]. Of note, in the present study we also found that SSc-MVECs challenged with MK-2947 showed an increase in gene expression of proangiogenic molecules and a decrease in

Fig. 5 Soluble guanylate cyclase stimulation attenuates the myofibroblast-like profibrotic and contractile phenotype of SSc-MVECs and effectively reduces ERK1/2 signalling

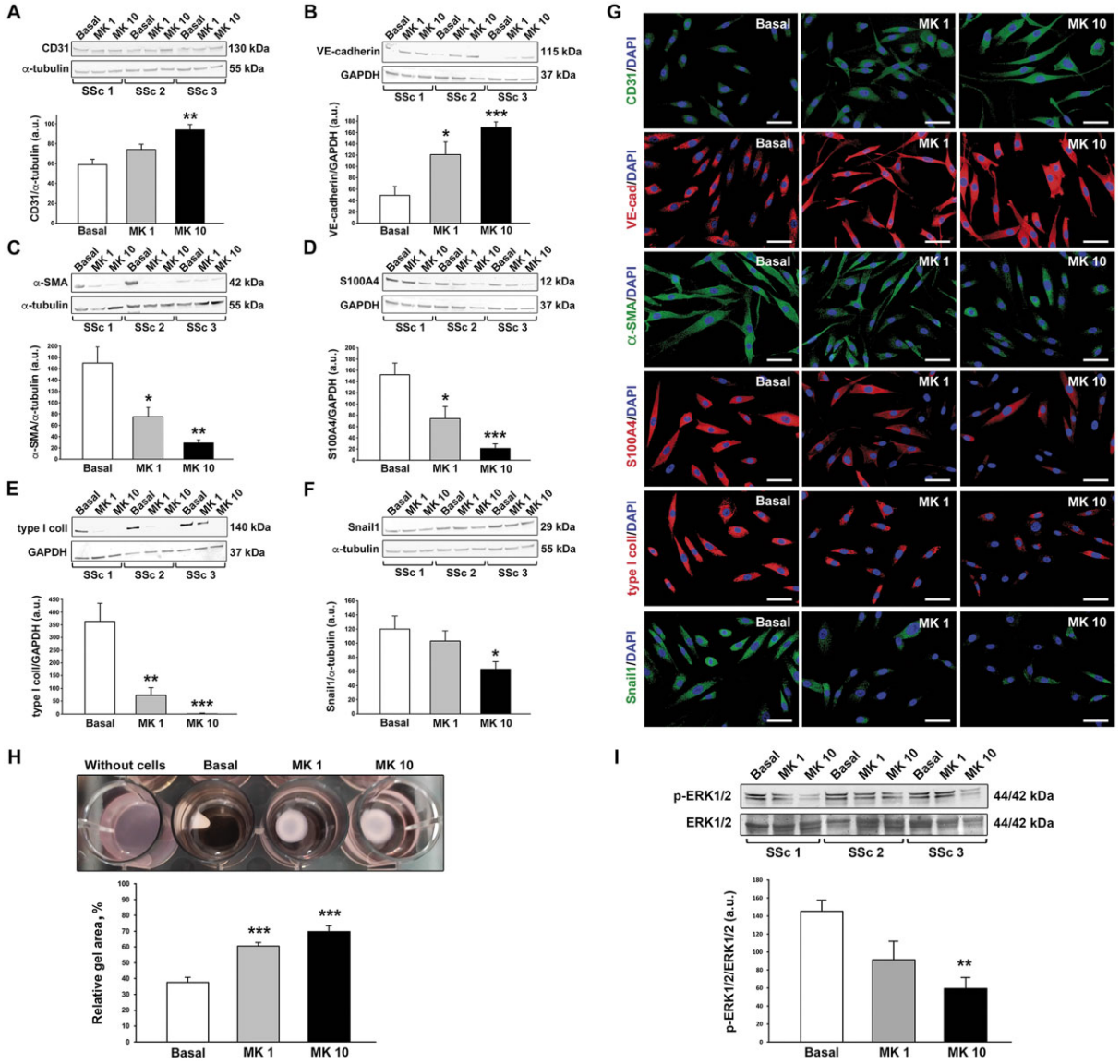

Experiments were performed on SSc-MVECs ($n = 5$) at basal condition and after treatment with MK-2947 1 μM or 10 μM. (**A**–**F**) Protein expression of CD31, VE-cadherin, α-SMA, S100A4, type I collagen and Snail1 assessed by immunoblotting, using α-tubulin (**A**, **C** and **F**) or GAPDH (**B**, **D** and **E**) as loading controls. Representative immunoblots are shown. Molecular mass values (kDa) are indicated. The densitometric analysis of the bands is reported in the bar graphs. Data are mean (S.E.M.) of optical density in arbitrary units (a.u.). (**G**) Representative fluorescence microphotographs of SSc-MVECs immunolabelled for CD31, VE-cadherin, α-SMA, S100A4, type I collagen and Snail1. Nuclei are counterstained with DAPI (blue). Scale bar = 50 μm. (**H**) Collagen gel contraction assay. Gels without cells were included as negative controls. Each experimental point was performed in triplicate. Bar graphs represent mean (S.E.M.) of gel size expressed as percentage of that observed in gel without cells. (**I**) Protein expression of p-ERK1/2 and total ERK1/2 assessed by immunoblotting. Representative immunoblots are shown. Molecular mass values (kDa) are indicated. The densitometric analysis of p-ERK1/2 bands normalized to total ERK1/2 is reported in the bar graphs. Data are mean (S.E.M.) of optical density in a.u. One-way ANOVA with *post hoc* Tukey's test was used for statistical analysis; $^{*}P < 0.05$, $^{**}P < 0.01$ and $^{***}P < 0.001$ *vs* basal. α-SMA: α-smooth muscle actin; DAPI: 4′,6-diamidino-2-phenylindole; ERK1/2, extracellular signal-regulated kinases 1 and 2; GAPDH, glyceraldehyde 3-phosphate dehydrogenase; MVEC: microvascular endothelial cell; VE-cadherin: vascular endothelial cadherin.

FIG. 6 Soluble guanylate cyclase stimulation counteracts SSc serum-induced EndoMT in H-MVECs

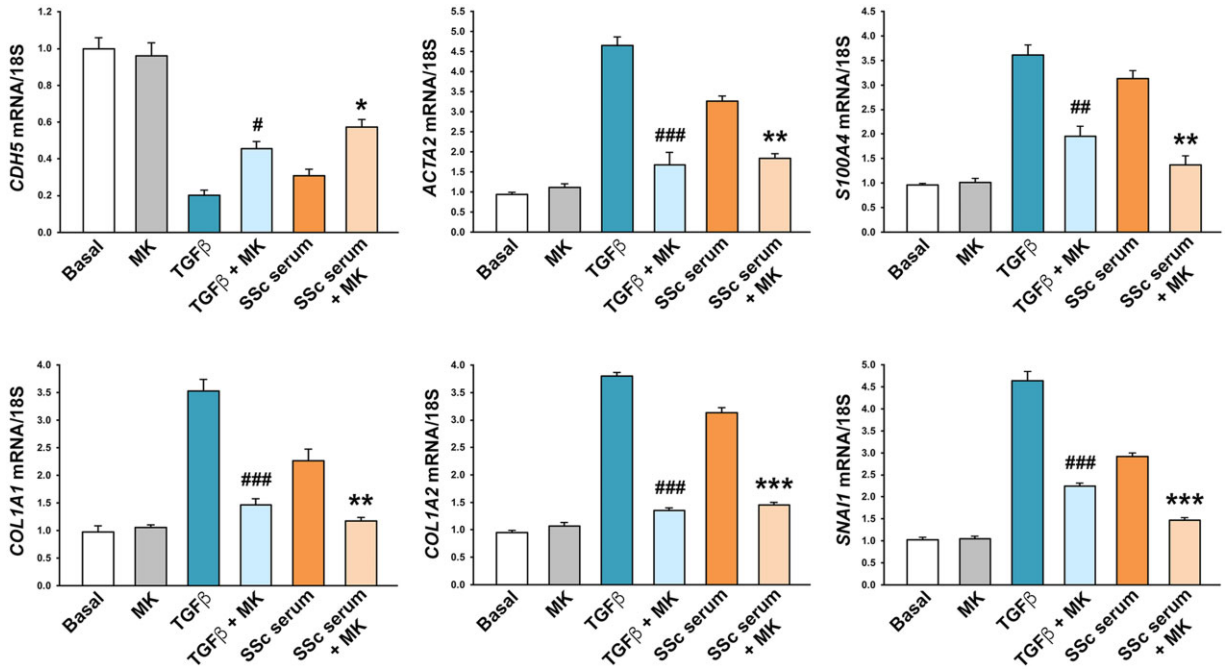

Gene expression of *CDH5*, *ACTA2*, *S100A4*, *COL1A1*, *COL1A2* and *SNAI1* was assessed by quantitative real-time PCR in H-MVECs ($n = 5$) at basal condition and after challenging with SSc sera ($n = 5$) or recombinant human TGFβ (positive control of EndoMT) preceded or not by treatment with MK-2947 10 μM. The basal level of each gene expression was set to 1. 18S rRNA was used as reference gene. Bars represent the mean (S.E.M.) of triplicate determinations. One-way ANOVA with *post hoc* Tukey's test was used for statistical analysis; $^{*}P < 0.05$, $^{**}P < 0.01$ and $^{***}P < 0.001$ *vs* SSc serum alone, $^{\#}P < 0.05$, $^{\#\#}P < 0.01$ and $^{\#\#\#}P < 0.001$ *vs* TGFβ alone. EndoMT: endothelial-to-mesenchymal transition; H-MVEC: healthy MVEC; MVEC: microvascular endothelial cell.

angiostatic factors, a result in accordance with previous reports showing that cGMP pathway activation may induce the synthesis of proangiogenic molecules including VEGF and MMP-9 [44–47].

The evidence that treatment with MK-2947 can efficiently blunt the profibrotic phenotype of SSc-MVECs also deserves in-depth discussion. Indeed, it is now recognized that endothelial cells may undergo EndoMT, thus representing an important source of myofibroblasts with pathogenic implications in both SSc-related microvascular dysfunction and fibrosis [7–9, 36]. Hence, depending on the type of affected microvessels, EndoMT may contribute either to fibroproliferative, occlusive vascular lesions or to decreased capillary density paralleling tissue fibrogenesis [8, 9]. Strikingly, an increase in cGMP following sGC stimulation/activation was shown to inhibit TGFβ-induced myofibroblast differentiation in human prostatic stromal cells and dermal and lung fibroblasts [19–22]. Moreover, riociguat was found to inhibit epithelial-to-mesenchymal transition in experimental renal fibrosis [13]. A strong antifibrotic effect of cGMP pathway activation was also reported in SSc both *in vitro* and in preclinical studies, where sGC stimulation inhibited fibroblast activation and blocked the development of skin fibrosis in SSc murine models [21–23]. Here, we have shown for the first time that the sGCS MK-2947 is able to counteract EndoMT not only in SSc-MVECs, but also in H-MVECs challenged with the principal EndoMT trigger, namely TGFβ. Moreover, in H-MVECs MK-2947 was also effective in counteracting the previously demonstrated pro-EndoMT effects of SSc sera [7]. Interestingly, we found that the MK-2947-mediated counteraction of SSc-MVEC profibrotic features was attributable to a reduction in phosphorylated-ERK1/2 protein levels, a finding fully consistent with previous evidence that pharmacological sGC stimulation is effective in inhibiting non-canonical, ERK-dependent TGFβ signalling both in dermal fibroblasts and in SSc experimental models [22, 23]. In perspective, further powerful deep-sequencing technologies, such as RNA-seq, might help to comprehensively decipher the transcriptional profile underlying changes in the myofibroblast-like phenotype and angiogenic potential of SSc-MVECs upon treatment with MK-2947.

Clinically, at present riociguat has demonstrated therapeutic efficacy in the treatment of SSc-related PAH [32, 48], a severe complication in whose pathogenesis EndoMT has remarkably been implicated [8, 49]. However, clinical trials performed so far on SSc patients did not reach their primary endpoints as far as improvement of skin involvement and DU healing are concerned [26, 34]. Nonetheless, it is worth considering that, when extending treatment duration, the same investigators reported potential efficacy signals, thus underlying the

need to investigate the effects of sGC stimulation for longer periods in additional clinical trials [26, 34]. In such a context, we believe that our promising *in vitro* findings not only provide new insights into the understanding of sGC stimulation's action on key pathogenetic mechanisms underlying SSc endothelial dysfunction, but also present new evidence for repurposing sGCSs for the treatment of SSc-related skin fibrosis and peripheral vascular manifestations.

Acknowledgements

E.R., M.M. and M.M.-C. contributed to the study planning and design. E.R., I.R., B.S.F., D.G., M.M. and M.M.-C. contributed to the analysis or interpretation of the data and critical revision of the manuscript. E.R., I.R. and M.M. drafted the manuscript. M.M. and M.M.-C. had access to all the data and act as guarantors for the study. All authors read and approved the final version of the manuscript.

Funding: This work was supported in part by a research grant from Investigator-Initiated Studies Program of Merck Sharp & Dohme, LLC and Bayer AG. The opinions expressed in this paper are those of the authors and do not necessarily represent those of Merck Sharp & Dohme, LLC and Bayer AG.

Disclosure statement: M.M.-C. has received consulting fees or honorarium from Merck Sharp & Dohme, Actelion, Janssen, Inventiva, Bayer, Biogen, Boehringer, CSL Behring, Corbus, Galapagos, Mitsubishi, Samsung, Regeneron, Acceleron, Chemomab, Lilly, Pfizer, Roche to him outside the submitted work. The other authors have declared no conflicts of interest.

Data availability statement

The data underlying this article are available in the article and in its online supplementary material.

Supplementary data

Supplementary data are available at *Rheumatology* online.

References

1 Varga J, Trojanowska M, Kuwana M. Pathogenesis of systemic sclerosis: recent insights of molecular and cellular mechanisms and therapeutic opportunities. J Scleroderma Relat Disord 2017;2:137–52.

2 Korman B. Evolving insights into the cellular and molecular pathogenesis of fibrosis in systemic sclerosis. Transl Res 2019;209:77–89.

3 Asano Y. The pathogenesis of systemic sclerosis: an understanding based on a common pathologic cascade across multiple organs and additional organ-specific pathologies. J Clin Med 2020;9:2687.

4 Manetti M, Guiducci S, Romano E *et al.* Overexpression of VEGF165b, an inhibitory splice variant of vascular endothelial growth factor, leads to insufficient angiogenesis in patients with systemic sclerosis. Circ Res 2011;109:e14–26.

5 Wang Y, Sun J, Kahaleh B. Epigenetic down-regulation of microRNA-126 in scleroderma endothelial cells is associated with impaired responses to VEGF and defective angiogenesis. J Cell Mol Med 2021;25:7078–88.

6 Romano E, Manetti M, Rosa I *et al.* Slit2/Robo4 axis may contribute to endothelial cell dysfunction and angiogenesis disturbance in systemic sclerosis. Ann Rheum Dis 2018;77:1665–74.

7 Manetti M, Romano E, Rosa I *et al.* Endothelial-to-mesenchymal transition contributes to endothelial dysfunction and dermal fibrosis in systemic sclerosis. Ann Rheum Dis 2017;76:924–34.

8 Romano E, Rosa I, Fioretto BS, Matucci-Cerinic M, Manetti M. New insights into profibrotic myofibroblast formation in systemic sclerosis: when the vascular wall becomes the enemy. Life (Basel) 2021;11:610.

9 Rosa I, Romano E, Fioretto BS, Manetti M. The contribution of mesenchymal transitions to the pathogenesis of systemic sclerosis. Eur J Rheumatol 2020;7:S157–64.

10 Sandner P. From molecules to patients: exploring the therapeutic role of soluble guanylate cyclase stimulators. Biol Chem 2018;399:679–90.

11 Friebe A, Sandner P, Schmidtko A. cGMP: a unique 2nd messenger molecule – recent developments in cGMP research and development. Naunyn Schmiedebergs Arch Pharmacol 2020;393:287–302.

12 Liu R, Kang Y, Chen L. Activation mechanism of human soluble guanylate cyclase by stimulators and activators. Nat Commun 2021;12:5492.

13 Stasch JP, Schlossmann J, Hocher B. Renal effects of soluble guanylate cyclase stimulators and activators: a review of the preclinical evidence. Curr Opin Pharmacol 2015;21:95–104.

14 Knorr A, Hirth-Dietrich C, Alonso-Alija C *et al.* Nitric oxide-independent activation of soluble guanylate cyclase by BAY 60-2770 in experimental liver fibrosis. Arzneimittelforschung 2008;58:71–80.

15 Xie G, Wang X, Wang L *et al.* Role of differentiation of liver sinusoidal endothelial cells in progression and regression of hepatic fibrosis in rats. Gastroenterology 2012;142:918–27.

16 Chen PJ, Kuo LM, Wu YH *et al.* BAY 41-2272 attenuates CTGF expression via sGC/cGMP-independent pathway in TGFβ1-activated hepatic stellate cells. Biomedicines 2020;8:330.

17 Kadoya H, Satoh M, Nagasu H, Sasaki T, Kashihara N. Deficiency of endothelial nitric oxide signaling pathway exacerbates peritoneal fibrosis in mice. Clin Exp Nephrol 2015;19:567–75.

18 Masuyama H, Tsuruda T, Sekita Y *et al.* Pressure-independent effects of pharmacological stimulation of

soluble guanylate cyclase on fibrosis in pressure-overloaded rat heart. Hypertens Res 2009;32:597–603.

19 Lambers C, Boehm PM, Karabacak Y *et al.* Combined activation of guanylate cyclase and cyclic AMP in lung fibroblasts as a novel therapeutic concept for lung fibrosis. Biomed Res Int 2019;2019:13 45402.

20 Zenzmaier C, Kern J, Heitz M *et al.* Activators and stimulators of soluble guanylate cyclase counteract myofibroblast differentiation of prostatic and dermal stromal cells. Exp Cell Res 2015;338: 162–9.

21 Beyer C, Reich N, Schindler SC *et al.* Stimulation of soluble guanylate cyclase reduces experimental dermal fibrosis. Ann Rheum Dis 2012;71:1019–26.

22 Beyer C, Zenzmaier C, Palumbo-Zerr K *et al.* Stimulation of the soluble guanylate cyclase (sGC) inhibits fibrosis by blocking non-canonical TGFβ signalling. Ann Rheum Dis 2015;74:1408–16.

23 Dees C, Beyer C, Distler A *et al.* Stimulators of soluble guanylate cyclase (sGC) inhibit experimental skin fibrosis of different aetiologies. Ann Rheum Dis 2015; 74:1621–5.

24 Yamamoto Y, Okano T, Yamada H *et al.* Soluble guanylate cyclase stimulator reduced the gastrointestinal fibrosis in bleomycin-induced mouse model of systemic sclerosis. Arthritis Res Ther 2021;23:133.

25 Armstrong PW, Pieske B, Anstrom KJ *et al.*; VICTORIA Study Group. Vericiguat in patients with heart failure and reduced ejection fraction. N Engl J Med 2020;382: 1883–93.

26 Nagaraja V, Spino C, Bush E *et al.* A multicenter randomized, double-blind, placebo-controlled pilot study to assess the efficacy and safety of riociguat in systemic sclerosis-associated digital ulcers. Arthritis Res Ther 2019;21:202.

27 Dasgupta A, Bowman L, D'Arsigny CL, Archer SL. Soluble guanylate cyclase: a new therapeutic target for pulmonary arterial hypertension and chronic thromboembolic pulmonary hypertension. Clin Pharmacol Ther 2015;97:88–102.

28 Sharkovska Y, Kalk P, Lawrenz B *et al.* Nitric oxide-independent stimulation of soluble guanylate cyclase reduces organ damage in experimental low-renin and high-renin models. J Hypertens 2010;28:1666–75.

29 Lang M, Kojonazarov B, Tian X *et al.* The soluble guanylate cyclase stimulator riociguat ameliorates pulmonary hypertension induced by hypoxia and SU5416 in rats. PLoS One 2012;7:e43433.

30 Schwabl P, Brusilovskaya K, Supper P *et al.* The soluble guanylate cyclase stimulator riociguat reduces fibrogenesis and portal pressure in cirrhotic rats. Sci Rep 2018;8:9372.

31 Ghofrani HA, Galiè N, Grimminger F *et al.* Riociguat for the treatment of pulmonary arterial hypertension. N Engl J Med 2013;369:330–40.

32 Humbert M, Coghlan JG, Ghofrani HA *et al.* Riociguat for the treatment of pulmonary arterial hypertension associated with connective tissue disease: results from PATENT-1 and PATENT-2. Ann Rheum Dis 2017;76:422–6.

33 Ghofrani HA, Hoeper MM, Halank M *et al.* Riociguat for chronic thromboembolic pulmonary hypertension and pulmonary arterial hypertension: a phase II study. Eur Respir J 2010;36:792–9.

34 Khanna D, Allanore Y, Denton CP *et al.* Riociguat in patients with early diffuse cutaneous systemic sclerosis (RISE-SSc): randomised, double-blind, placebo-controlled multicentre trial. Ann Rheum Dis 2020;79:618–25.

35 van den Hoogen F, Khanna D, Fransen J *et al.* 2013 classification criteria for systemic sclerosis: an American College of Rheumatology/European League against Rheumatism collaborative initiative. Arthritis Rheum 2013; 65:2737–47.

36 Corallo C, Cutolo M, Kahaleh B *et al.* Bosentan and macitentan prevent the endothelial-to-mesenchymal transition (EndoMT) in systemic sclerosis: in vitro study. Arthritis Res Ther 2016;18:228.

37 Saygin D, Highland KB, Tonelli AR. Microvascular involvement in systemic sclerosis and systemic lupus erythematosus. Microcirculation 2019;26:e12440.

38 Romano E, Rosa I, Fioretto BS *et al.* A new avenue in the pathogenesis of systemic sclerosis: the molecular interface between the endothelial and the nervous systems. Clin Exp Rheumatol 2019;37:133–40.

39 Pyriochou A, Beis D, Koika V *et al.* Soluble guanylyl cyclase activation promotes angiogenesis. J Pharmacol Exp Ther 2006;319:663–71.

40 Morbidelli L, Pyriochou A, Filippi S *et al.* The soluble guanylyl cyclase inhibitor NS-2028 reduces vascular endothelial growth factor-induced angiogenesis and permeability. Am J Physiol Regul Integr Comp Physiol 2010; 298:R824–32.

41 Yamamoto K, Nishimura R, Kato F *et al.* Protective role of endothelial progenitor cells stimulated by riociguat in chronic thromboembolic pulmonary hypertension. Int J Cardiol 2020;299:263–70.

42 Zagorski J, Neto-Neves E, Alves NJ, Fisher AJ, Kline JA. Modulation of soluble guanylate cyclase ameliorates pulmonary hypertension in a rat model of chronic thromboembolic pulmonary hypertension by stimulating angiogenesis. Physiol Rep 2022;10:e15156.

43 Dhahri W, Dussault S, Desjarlais M *et al.* Stimulation of soluble guanylate cyclase activity with riociguat promotes angiogenesis and improves neovascularization after hindlimb ischemia [abstract]. Circulation 2016;134: A15850.

44 Coletta C, Papapetropoulos A, Erdelyi K *et al.* Hydrogen sulfide and nitric oxide are mutually dependent in the regulation of angiogenesis and endothelium-dependent vasorelaxation. Proc Natl Acad Sci USA 2012;109: 9161–6.

45 Gomes de Almeida Schirmer B, Crucet M, Stivala S *et al.* The NO-donor MPC-1011 stimulates angiogenesis and arteriogenesis and improves hindlimb ischemia via a cGMP-dependent pathway involving VEGF and SDF-1α. Atherosclerosis 2020;304:30–8.

46 Marcet-Palacios M, Graham K, Cass C *et al.* Nitric oxide and cyclic GMP increase the expression of matrix metalloproteinase-9 in vascular smooth muscle. J Pharmacol Exp Ther 2003;307:429–36.

47 Ridnour LA, Windhausen AN, Isenberg JS *et al.* Nitric oxide regulates matrix metalloproteinase-9 activity by guanylyl-cyclase-dependent and -independent pathways. Proc Natl Acad Sci USA 2007;104:16898–903.

48 Bruni C, Guignabert C, Manetti M, Matucci-Cerinic M, Humbert M. The multifaceted problem of pulmonary arterial hypertension in systemic sclerosis. Lancet Rheumatol 2021;3:e149–59.

49 Good RB, Gilbane AJ, Trinder SL *et al.* Endothelial to mesenchymal transition contributes to endothelial dysfunction in pulmonary arterial hypertension. Am J Pathol 2015;185:1850–8.